PRINTABILITY OF THERMOPLASTIC POLYURETHANE WITH LOW SHORE A HARDNESS IN THE CONTEXT OF CUSTOMIZED INSOLES PRODUCTION

Mariana Cristiana IACOB[1], Diana POPESCU[2], Tudor George ALEXANDRU[3]

This article explores the printability of thermoplastic polyurethane (TPU) with 60A and 70A shore hardness by Material Extrusion-based Additive Manufacturing for orthotics applications. It highlights challenges in fine-tuning TPU printing parameters such as temperature, nozzle diameter, and flow ratio, to address and mitigate nozzle clogs, filament buckling, jams, and poor print quality issues. As literature lacks guidance in this area, this paper fills the gap by providing insights into the calibration methods, as well as recommendations on parameter settings for these materials. Additionally, it presents a case study that includes the design, manufacturing and testing of customized insole with variable infill stiffness based on acquired expertise on 3D printing low shore A filaments, hardness measurements and plantar pressure evaluation. The main findings showed that insoles with good cushion properties can be produced from highly flexible filaments, if careful attention is given to the specific aspects outlined in the study.

Keywords: 3D printing, thermoplastic polyurethane, TPU 60A, TPU 70A, insoles design, variable stiffness, plantar pressure, FEA

1. Introduction

Material extrusion-based process (MEX) has traditionally been used to produce rigid components, with polylactic acid (PLA) and acrylonitrile butadiene styrene (ABS) being among the commonly employed materials. More recently, filaments based on carbon, glass or Kevlar were developed for manufacturing parts that exhibit enhanced mechanical properties, particularly in terms of tensile, compressive, and flexural strength [1]. Extensive studies have been conducted on such rigid materials, exploring their printability, surface quality, dimensional and form accuracy, and mechanical performance, in correlation with process parameter settings. However, certain applications demand the use of flexible

[1]PhD Student, Dept.of Robotics and Production Systems, National University of Science and Technology POLITEHNICA Bucharest, Romania, e-mail: mariana.iacob@stud.fiir.upb.ro
[2] Prof., Dept.of Robotics and Production Systems, National University of Science and Technology POLITEHNICA Bucharest, Romania, e-mail: diana.popescu@upb.ro
[3] Lecturer, Dept.of Robotics and Production Systems, National University of Science and Technology POLITEHNICA Bucharest, Romania, e-mail: tudor.alexandru@upb.ro

materials, such as thermoplastic polyurethane (TPU), in the manufacturing of products like insoles, wearables, tires, grippers or hinges [7]. In such cases, the objectives are to adjust stiffness, combine thermoplastic polyurethane (TPU) with rigid polymers, improve surface quality, and produce defect-free products [8]. These can be achieved by using TPU with different shore A hardness and/or by parameter settings [9]. varioShore filaments (Colorfabb, NL), for instance, based on TPU 92A material and active foaming agent, allow changing the density and hardness of a print by adjusting printing temperature, flow or printing speed [9].

Hands-on experience with 3D printing TPU highlighted challenges of fine-tuning parameters such as printing temperature, flow, retraction, and deposition speed. Filaments with low TPU hardness poses significant challenges in establishing appropriate process parameters for preventing defects and ensuring good accuracy and surface quality. Managing these parameters proves particularly difficult due to the material's flexible characteristics, resulting in issues such as buckling, nozzle clogs, burrs, void spaces, and stringing.

Existing literature lacks detailed guidance on how to avoid extensive testing and calibration processes, leading to material waste and time consumption. This is particularly evident for low shore A hardness filaments (60A or 70A). Within this context, the research aims to fill this knowledge gap by presenting a calibration methodology, optimal parameter configurations, g-code adjustments, and practical recommendations. Also, the paper includes a case study demonstrating the application of this knowledge in producing customized foot orthoses (insoles) with variable stiffness from TPU 60A filament.

2. Materials and methods

The experimental procedures were conducted using Original Prusa i3 MK3S+ 3D printer equipped with an E3D Revo extruder (Fig. 1a). Specifically, TPU 60A and TPU 70A (Filaflex brand, Recreus, ES), the softest filaments available on the market (Filaflex 60A - 950% elongation at break, Filaflex 70A - 900% elongation at break), were selected to prioritize the insoles' comfort factor.

2.1. 3D printing challenges and mitigation strategies by parameter settings

Given the high hygroscopic nature of TPU, ensuring proper tension adjustment of the extruder gears, as well as using a dehydrator for filament (at least 12h prior to 3D printing at 55°C) were mandatory tasks to perform before starting the 3D printing process [9] (Fig. 1a). Insufficiently dried filaments can lead to the break of polymer chains when the material undergoes heating for extrusion. This results in significant quality issues during manufacturing (Fig. 1b).

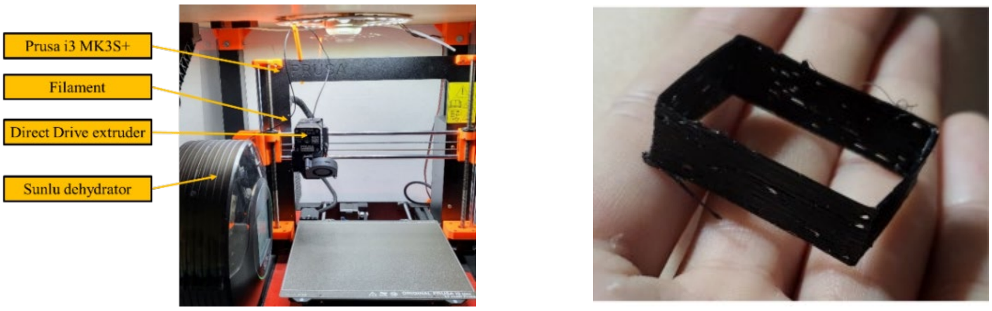

a. b.

Fig. 1. 3D Printing low shore hardness filament (FilaFlex 70A), set-up configuration (a), and defects caused by lack of dehydration (b)

Below are discussed additional common issues that may arise when 3D printing low shore A hardness filaments:

- Incorrect insertion of the filament into the hotend can occur due to possible gaps between the filament drive wheels and its entry port, leading to filament jams or buckling (Fig. 2);
- Excessive friction between the low shore A filament and the interior of the nozzle is a significant challenge, primarily caused by thermal expansion of the filament and the subsequent high material adhesion to the inner nozzle walls. To address this issue, one potential solution is to use a one-body brass nozzle design like the E3D Revo, which can help mitigate these challenges effectively;
- The diameter of the nozzle significantly impacts the pressure within the hotend. When the pressure increases excessively, nozzle clogging can result. There is an inverse relationship between the nozzle diameter and the pressure build-up inside it, so careful calibration of the flow ratio is essential.

Considering the likelihood of encountering the discussed challenges, conducting thorough calibration tests was mandatory. Rectangular and cubic calibration prints (30 mm x 20 mm x 10 mm with a thickness of 0.65 mm, respectively 10 mm x 10 mm x 10 mm x 10 mm x 10 mm x 10 mm) were used. Tests were conducted with nozzles with 0.4 mm and 0.6 mm diameters, in association with settings of printing temperature, flow ratio and fan speed:

a) Nozzle of 0.4 mm diameter

For different printing temperature values (215°C, 220°C, 228°C, 230°C, 235°C) and customizing cooling for the smaller dimensions of the parts, good quality and accuracy prints were obtained (tolerances of ± 0.05 mm – rectangular specimens, and ± 0.1 mm – cubes) both for Filaflex 60A (fig. 3a) and Filaflex 70A (fig. 3b) – more information in section 3.1 and table 1.

b) Nozzle of 0.6 mm diameter

Following similar calibration tests (Fig. 4), it was noted that 0.6 mm diameter nozzle facilitates easier calibration and produces less frequent nozzle clogging. Consequently, the insoles were produced using the 0.6 mm nozzle.

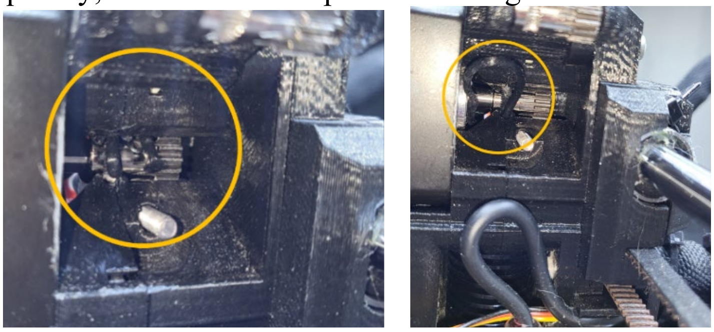

a. b.

Fig. 2. Filament problems caused by the highly flexible nature of the filaments: (a) jam in the extruder - Filaflex 60A at 215°C; (b) filament buckling.

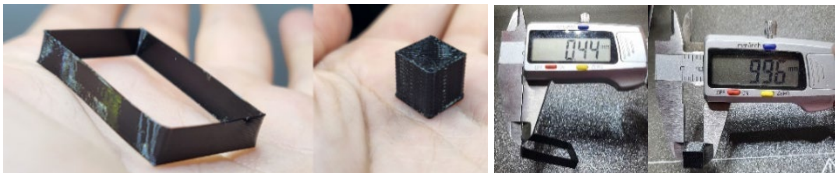

a.

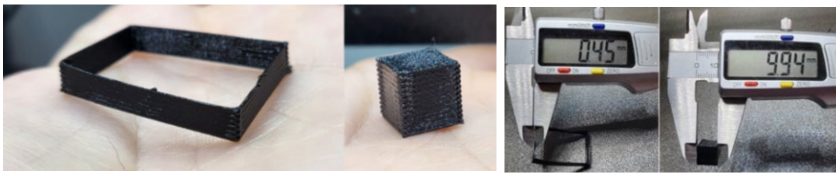

b.

Fig. 3. Calibration tests– nozzle of 0.4 mm diameter: (a) Filaflex 60A (230 °C - first layer; 225 °C - other layers); (b) Filaflex 70A (228 °C - all layers)

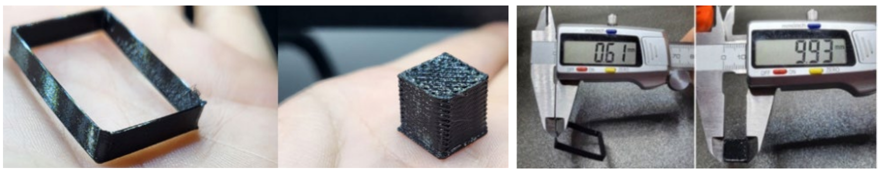

a.

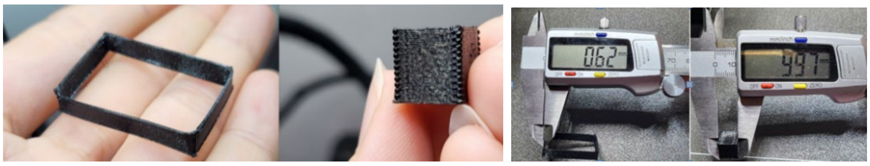

b.

Fig. 4. Calibration tests – nozzle of 0.6 mm diameter: (a) Filaflex 60A; (b) Filaflex 70A

The following observations can be summarized regarding the tested printing temperatures:

- 215 °C - causes jam in the extruder as shown in Fig. 2.
- 220 °C – causes a degraded quality of surfaces;
- 228 °C – ideal for Filaflex 70A, after numerous tests, the accuracy of dimensions and quality of surfaces proved good;
- 230 °C – ideal for first layer for Filaflex 60A, and for other layers the temperature can be 225 °C;
- 235 °C – causes a degraded quality of surfaces.

2.2. Insoles design process

In this study, a flat design model of the insole was considered for improving the comfort level of the user (cushion performance). Therefore, the insole was 6 mm in thickness to provide comfort without compromising its fit inside the shoe.

A critical aspect in such application is represented by the plantar pressure. This pressure is exerted by the foot onto the supporting surface, both during walking and stationary activities [10-11]. This pressure is not uniformly distributed across the entire sole, certain areas, such as the heel and the forefoot usually experience higher pressure due to biomechanical and physiological factors such as weight distribution, toe-off movement or heel initial contact with the ground during walking, push-off during propulsion phase, etc. [12]. Considering this observation, 3D scans of both the left and right foot were conducted to evaluate the distribution of the peak plantar pressure, which is particular to each individual. Scanning was carried out using the Artec Eva Lite handheld 3D scanner (Artec Inc., USA). Subsequently, the scans underwent processing in Meshmixer, and then converted into STL format to facilitate their use in the 3D printing process (Fig. 5). The necessary adjustments for areas with peak plantar pressure were obtained using the Prusa Slicer software based on the data acquired using a clay model. The STL files of both feet were imported into the slicer as modifier bodies and positioned beneath the XY plane (Fig.6) with a value approximately 20-21% of the overall dimension (about 5mm).

By intersecting the scanned model of the foot with the insole's model, the areas for modifying the infill density and infill pattern of the model were generated. The scan was interpreted by the slicer as a mesh modifier, enabling targeted alterations to the 3D printing process. For these modifications, separate commands can be directly input into the g-code file used on modifier bodies, as it is shown in fig. 7.

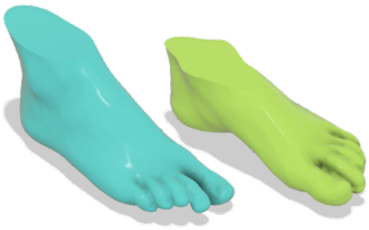

Fig. 5. 3D models of the feet

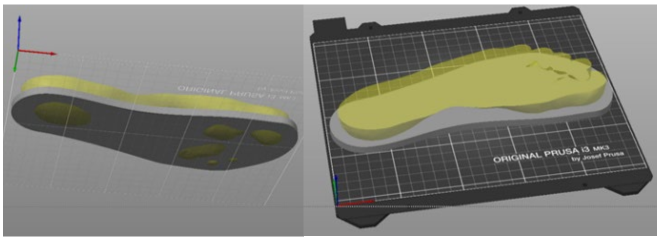

Fig. 6. Prusa Slicer – modifier body

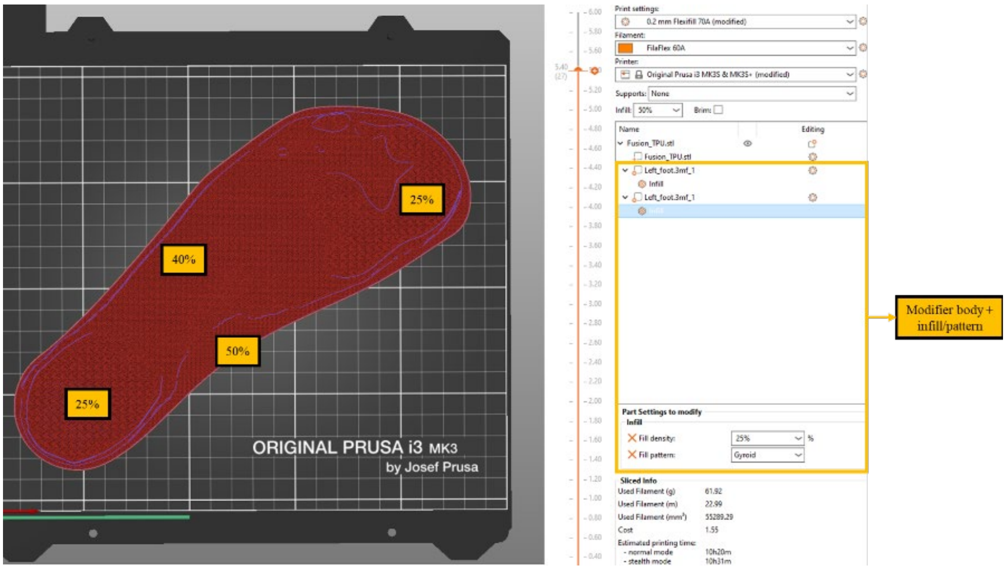

Fig. 7. Prusa Slicer - modified areas – left foot

2.3. Peak plantar pressure evaluation method

In this study, to correctly identify the high plantar pressure zones of the feet of a healthy user, a novel method of evaluation was used, as further presented. Gather data was then input in Prusa Slicer and variable infill density g-code was generated.

Two molds were designed (fig. 8a), one for each foot, followed by their 3D printing using PETG filament (fig. 8b). These molds helped placing in the clay so that to ensure having the same amount of material in both forms (10 mm height) as shown in fig. 8c. After the clay foot printing process, the molds went into an oven at 60 °C for about 3 h (fig. 8d). The subsequent step involved removing the solidified clay from the molds and subjecting them to full hardening in the oven at 150 °C for 30 minutes, as shown in figure 8e. Both impressions were 3D scanned with RevoPoint Mini 3D scanner (RevoPoint, Shenzhen, Guangdong, China) and processed with dedicated software Revo Scan 5.

Fig 8. Peak plantar pressure evaluation process: a) 3D modeling the molds; b) 3D-printed molds; c) Clay forming; d) Baking ready molds; e) Fully hardened clay.

The plantar pressure was evaluated by determining the elastic constant of the clay employed in the design of the mold. In this regard, variable compressive loads were applied for capturing the displacement, based on equation (1):

$$F = -k \cdot x \tag{1}$$

where: F represents the applied compressive force and k is the unknown elastic constant resulting from the x value of the displacement.

In the next stage, a Fortran program was developed for processing the reaction forces from the STL file. For each vertex, the Z coordinate indicated the base frame offset. The maximum Z coordinate value was used as a reference for calculating the displacement of all points. Each vertex was linked to multiple elements. Thus, the plantar pressure was derived by dividing the calculated loads to simple fractions of the areas associated with a vertex. The process was carried out for all elements.

3. Results and discussions

3.1. 3D printing insoles process parameter settings

After conducting calibration tests with various parameter settings, the values presented in Table 1 are recommended and were employed specifically with Filaflex 60A and Filaflex 70A for manufacturing the insoles. Highlighted in table 1, second column, are the optimal printing temperatures. It is important to note that the calibration process needs to be individually carried out by every operator on own 3D printer. The values presented in Table 1 are specifically configured for the Original Prusa i3 MKS+ 3D printer equipped with the E3D Revo extruder. While the calibration takes time, it guarantees high-quality and accurate prints. Additionally, the settings establish a profile that operators can consistently apply when using filaments with extremely high flexibility.

Table 1

Recommended settings parameters for printing Filaflex 60A and 70A.

Material	**Printing temp. [°C]**	**Bed temp. [°C]**	**Printing speed [mm/s]**	**Flow material [%]**	**Fan speed [%]**
Filaflex 60A	**First layer: 230** **Other layers: 225**	0	20	100	50 Disable for first 3 layers
Filaflex 70A	**228**	0	20	100	50 Disable for first 3 layers

To determine the hardness of the insoles made with different configurations of the parameter settings in Table 1, eight square samples with dimensions of 40 mm x 40 mm x 6 mm were 3D printed (Fig. 9), and their hardness was measured using a durometer (Table 2). These values were corroborated with the results of peak plantar pressure evaluation for customizing the values of the insoles' infill density for each foot zone.

The hardness measurement results were calculated as the average of ten random points measured on each sample. Gyroid and cubic patterns were used for the samples, with infill densities set at 30%, 40%, 50%, and 60%.

Fig. 9. Filaflex 60A – samples and measurement with Shore A durometer

Table 2

3D printing settings used for insoles production – Filaflex 60A.

Sample size [mm x mm x mm]	Item	Pattern	Infill density [%]	Weight [g]	Shore A hardness
40 x 40 x 6	1	Cubic	30	2.89	8.6
	2		40	3.10	10.3
	3		50	3.71	20.75
	4		60	4.42	26.55
	5	Gyroid	30	3.40	15.65
	6		40	3.97	24.65
	7		50	4.50	28.85
	8		60	5.19	35.85

3.2. Peak plantar pressure results

The models obtained through the process detailed in section 2.3 underwent post-processing for thickness analysis and assessment using SolidWorks 2022 (Dassault Systèmes SE, France), as illustrated in figure 10a.

After analyzing the results, it was noted that the most significant deformation for the right foot insole measured 9.47 mm, and for the left foot insole, it measured 9.6 mm. These values were recorded specifically in the heel area for both insoles. Toes zone also recorded high plantar pressure, but not the metatarsophalangeal area which recorded less pressure (yellow areas). Blue zones of the feet indicate very little plantar pressure in the arch zone.

Table 3 summarizes the main stiffness parameters, while figure 10b depicts the pressure plot for right and left foot insole.

A linear approximation is derived for describing the relationship between the measured displacement and the elastic constant as:

$$k = 1.131 \cdot \mathrm{x} + 4.7501 \qquad (2)$$

The external data interface from ANSYS Workbench 19.0 was employed for visualization purposes. In both cases the maximum pressure was concentrated in the big toe and the heel areas. A difference of 8.7% can be noticed in the magnitude of the two plots. This behavior is in accordance with section 2.2.

Table 3

Elastic constant values derived at different compressive loads.

F [N]	k [N/mm]	x [mm]
3.76	30	7.97
5.06	60	11.85
8.75	125	14.28

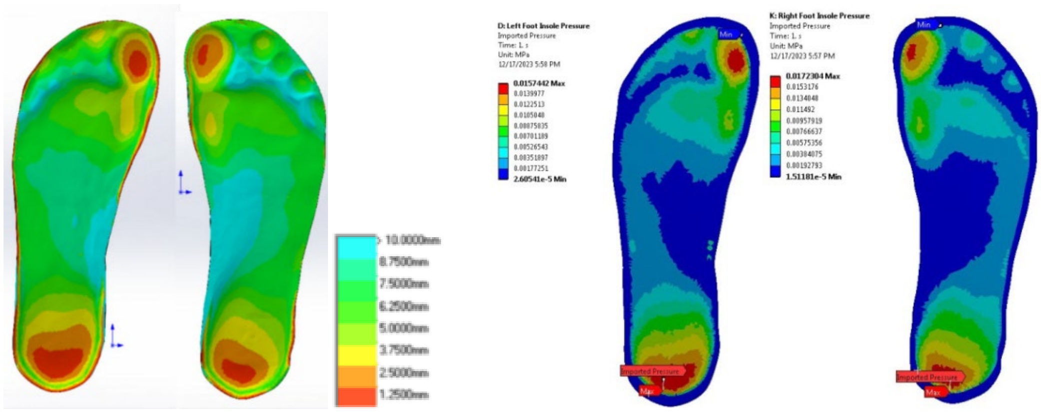

a) b)

Fig. 10. Thickness analysis with SolidWorks 2022 (a) vs. ANSYS plantar pressure plot for left and right foot insole (b)

3.3. 3D printing the insoles

Table 4 presents the settings for the main printing parameters used for insoles production.

Table 4

3D printing settings used for insoles production – Filaflex 60A

Printing settings	Values
Printing temperature [°C]	First layer: 230; Other layers: 225
Bed temperature [°C]	0
Printing speed [mm/s]	20 – bridges, top solid infill; 25
Flow material [%]	1.03
Layer height [mm]	0.2
Top/bottom layers	3/2
Infill density and pattern	Sample 1: Gyroid, 50%
	Sample 2: Gyroid 25% highest pressure zones, 40% and 50% the other zones (see fig. 7)

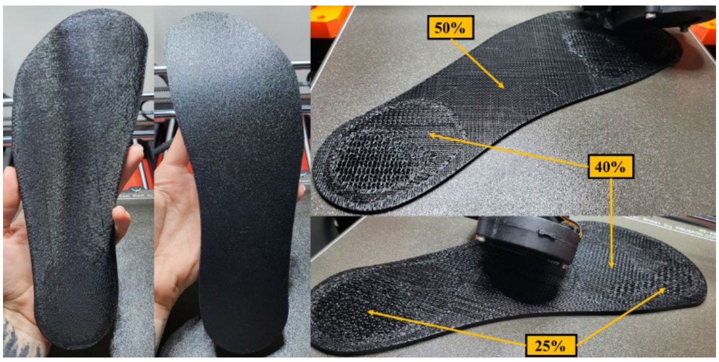

Fig. 11. Filaflex 60A - Left foot insole sample (25%, 40%, 50% infill densities)

Two samples were produced for each foot and then tested for comfort. The infill density values for the customized insoles were established based on the peak plantar pressure evaluation (fig.10b), as well as on the hardness values (fig. 3, table 2): the higher the pressure, the lower the thickness of the clay model.

Figure 11 shows images from the left insoles 3D printing process, the values of infill density being specified for different zone of the foot based on plantar pressure assessment.

3.4. User experience evaluation

The insoles were tested at walking, standing and jumping for about one hour in total.

Both types of insoles were tested by the healthy user whose footprints were used as model, the feedback favoring samples 2, although samples 1 were also considered comfortable:

- Sample 1: The insole's hardness was suitable, allowing easy bending within the shoe while maintaining a smooth top surface. It effectively sustained body weight, but due the uniform infill density, it lacked adequate protection for higher pressure areas of the foot;
- Samples 2: The insole's hardness was ideal. Similar to sample 1, it also enabled easy bending within the shoe and maintaining a smooth top surface. It effectively supported body weight, with the lower density infill providing support to the heel and toe areas, resulting in better pressure distribution and balance across the entire insole.

4. Conclusions and further work

The study focused on examining the viability of using flexible thermoplastic polyurethane materials, rated with 60A and 70A shore hardness, for orthotic purposes, specifically in producing customized foot orthoses (insoles) by material extrusion process. The challenges associated with 3D printing extremely flexible filaments, discussing and outlining methods to mitigate these issues were also covered considering the lack of such practical information in the literature. Moreover, optimal 3D printing settings for Filaflex 60A and 70A and the considered printer and extruder, were established ensuring the accuracy and quality of prints. These were used to produce customized insoles with variable infill densities based on hardness measurements for different parameter settings, as well as on peak plantar pressure analysis based on the use of a clay model, validated by a finite element analysis. The feedback from users indicated the effectiveness of the chosen material and the plantar pressure measurement technique. However, further study will be focused on a more precise calibration of the peak plantar pressure and infill density values by conducting mechanical compression tests.

REFERENCES

[1] *S.H.R.Sanei, D. Popescu,* "3D-Printed Carbon Fiber Reinforced Polymer Composites: A Systematic Review", Journal of Composite Science, **vol. 4**, 98, 2020, https://doi.org/10.3390/jcs4030098

[2] *M.C. Iacob, D. Popescu, D. Petcu, R. Marinescu, "*Assessment of the Flexural Fatigue Performance of 3D-Printed Foot Orthoses Made from Different Thermoplastic Polyurethanes", Applied Sciences, **vol. 13**, no. 22, 12149, 2023. https://doi.org/10.3390/app132212149

[3] *S. Kumar, R. Singh, A. P. Singh, Y. Wei,* "Three-dimensional printed thermoplastic polyurethane on fabric as wearable smart sensors", Proceedings of the Institution of Mechanical Engineers, Part L: Journal of Materials: Design and Applications, **vol. 237**, 1678–1692, 2023. https://doi.org/10.1177/14644207221149693

[4] *Y. Tao, J. Z. Shao, P. Li, S. Q. Shi,* "Application of a Thermoplastic Polyurethane/Polylactic Acid Composite Filament for 3D-Printed Personalized Orthosis", Materiali in tehnologije, **vol. 53**, no. 1, 71–76, 2019. https://doi.org/10.17222/mit.2018.180

[5] *J. Wang, B. Yang, X. Lin, L. Gao, T. Liu, Y. Lu, R. Wang,* "Research of TPU Materials for 3D Printing Aiming at Non-Pneumatic Tires by FDM Method", Polymers, **vol. 12**, no.11, 2492, 2020. https://doi.org/10.3390/polym12112492

[6] *C. Tawk, R. Mutlu, G. Alici,* "A 3D Printed Modular Soft Gripper Integrated With Metamaterials for Conformal Grasping", Frontiers in Robotics and AI, **vol. 8**, 2022. https://doi.org/10.3389/frobt.2021.799230

[7] *F. Rosa; M. Bordegoni, A. Dentelli, A. Sanzone, A. Sotgiu,* "Print-In-Place of Interconnected Deformable and Rigid Parts of Articulated Systems", Procedia Manufacturing, **vol. 11**, 555–562, 2017. https://doi.org/10.1016/j.promfg.2017.07.149

[8] *L. Rodríguez, G. Naya, R. Bienvenido,* "Study for the selection of 3D printing parameters for the design of TPU products", *IOP Conference Series: Materials Science and Engineering*, Gijón, Spain, **vol. 1193**, 012035, 2021. https://doi.org/10.1088/1757-899x/1193/1/012035

[9] *M.C. Iacob, D. Popescu, F. Baciu, Effect of process parameters on the hardness of 3D-printed thermoplastic polyurethane that includes foaming agent,* Materiale Plastice, **vol.60**, no.4, 144-154, 2023. https://doi.org/10.37358/mp.23.4.5694

[10] *Z. Ma, J. Lin, X. Xu, Z. Ma, L. Tang, C. Sun, D. Li, C. Li, Y. Zhong, L. Wang,* "Design and 3D Printing of Adjustable Modulus Porous Structures for Customized Diabetic Foot Insoles", International Journal of Lightweight Materials and Manufacture, **vol. 2**, no. 1, 57 - 63, 2019. https://doi.org/10.1016/j.ijlmm.2018.10.003

[11] *S. Shaikh, B. Jamdade, A. Chanda,* "Effects of Customized 3D-Printed Insoles in Patients with Foot-Related Musculoskeletal Ailments—A Survey-Based Study", Prosthesis, **vol. 5**, no. 2, 550-561, 2023. https://doi.org/10.3390/prosthesis5020038

[12] *A. Segal, E. Rohr, M. Orendurff, J. Shofer, M. O'Brien, B. Sangeorzan B*, "The Effect of Walking Speed on Peak Plantar Pressure", Foot & Ankle International, 25(12), 926-933, 2004. https://doi.org/10.1177/107110070402501215